

## ANALYSIS AND SIMULATION OF REENRANT CYLINDRICAL CAVITIES

Joaquim J. Barroso, Pedro J. Castro, Joaquim P. Leite Neto, and  
Odylio D. Aguiar

*Associated Plasma Laboratory,  
National Institute for Space Research—INPE  
P.O. Box 515, São José dos Campos, 12245-970 SP, Brazil*

Received 6 June 2005

### Abstract

Of applications ranging from electron spin resonance to detection of gravitational waves, reentrant circular cylindrical cavities are analyzed on the basis of a mathematically simple formalism extending the range of validity of expressions for resonant frequency and quality factor obtained from lumped RLC constant models. Several cavity configurations in the 1 - 3 GHz range are analytically examined in excellent agreement with frequencies obtained from Superfish code.

**Keywords:** reentrant cylindrical cavities, klystron resonant cavities, tunable resonators, electromechanical transducers.

### 1. Introduction

Having a simple mechanical construction and wide tuning range, narrow gap reentrant cylindrical cavities were originally investigated during the development years of the klystron [1,2] and have since then been widely used for the construction of microwave oscillators. These cavities allow the realization of resonant frequencies in the low GHz range without the need for large physical dimensions, with the ridged gap having the effect of reducing the frequency and focusing the electric field (Fig.1). By providing a well-defined electric field in the gap region, such cavities also find application in particle accelerators [3], solid-state microwave oscillators [4], tunable resonators [5], characterization of dielectrics [6],

measurement of semiconductor parameters [7], microwave scanning microscopy [8], electron spin resonance spectroscopy [9], susceptibility measurements [10], microwave tubes [11], and electromechanical sensors of gravitational waves [12].

Since the exact solutions of Maxwell's equations inside the cavity configuration are not known, the properties of interest (resonant frequency, quality factor) cannot be calculated exactly. The accuracy of these calculations is limited by how well one can approximate the fringing fields near the gap. Some models include a simple equivalent circuit [13-16], usually a TEM coaxial line loaded by a capacitive gap in which the fringing fields are matched on the cylindrical boundary surface at the inner radius  $r_1$  (Fig.1) provided the cavity is neither too flat nor too long. On the other hand, more accurate models [16-19] calculate the admittances of the gap and lateral regions from the equivalent magnetic current using Green's functions, thereby entailing involved formulas and heavy computation. In the light of such considerations, the present paper proposes a mathematically simple engineering solution for the problem by deriving a frequency equation encompassing expressions that are accurate enough only for small and large gap spacings. Several cavity configurations are examined in the 1-3 GHz range with excellent agreement being found between the frequencies predicted analytically and those obtained with the numerical code Superfish [20].

## 2. Cavity Analysis

As pictured in Fig. 1, at a small gap spacing the electric field lines run from one plate to the other, with an electric field concentration above the ridge. For such axisymmetric and lowest order operating mode ( $TM_{010}$ ), an accurate analysis can be made as the gap spacing gets small compared with the other dimensions of the cavity and with the resonant wavelength  $\lambda_0$ . In this condition the concept of lumped circuit elements becomes meaningful, whereby the reentrant cavity can be treated as shorted coaxial line terminated by a capacitor.

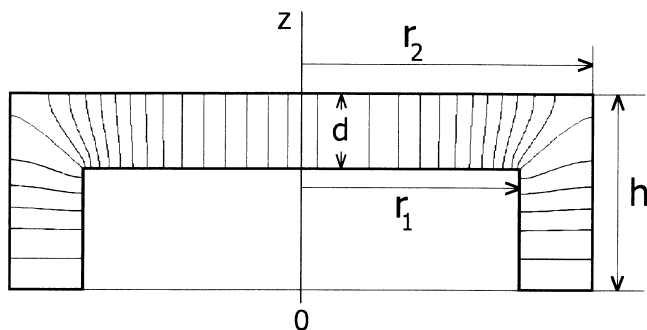


Fig. 1. Reentrant cavity schematic showing electric field lines.

Then assuming  $2\pi h/\lambda_0 \ll 1$ , the resonant frequency is obtained as [12,13]

$$f_0(d) = \frac{\sqrt{2} c}{2\pi r_1} \frac{\sqrt{d/h}}{\sqrt{\ln(r_2/r_1)}} \tag{1}$$

where  $c$  is the speed of light. In the other limit at the maximum gap size  $d/h=1$ , the geometry reduces to a circular  $TM_{010}$ -mode hollow cavity with resonant frequency

$$f_{TM} = \frac{c \chi}{2\pi r_2} \tag{2}$$

with  $\chi=2.4048$ , the first zero of the Bessel function  $J_0(\chi)$ . Then we seek a unifying expression that connects the two asymptotic regions. A suitable expression found is

$$f(d) = \frac{\chi c}{2\pi r_2} \frac{1 - \exp(-\nu \sqrt{d/h})}{1 - \exp(-\nu)} \tag{3}$$

where the parameter  $\nu$  is a function of the cavity dimensions, but having a very weak dependence on the ratio  $d/h$ . Setting  $d/h=1$  recovers (2), and in the small gap region the square root dependence  $\sqrt{d/h}$  remains

preserved, i. e. in the limit  $\nu\sqrt{d/h} \ll 1$  the numerator term in (3) reduces to  $\nu\sqrt{d/h}$ . To find  $\nu$ , we equate (1) and (3) to obtain

$$\frac{a[1 - \exp(-\nu)]}{1 - \exp(-\nu a)} = \frac{\chi}{\sqrt{2}} \frac{\sqrt{\ln(r_2/r_1)}}{r_2/r_1} \quad (4)$$

with  $a = \sqrt{d/h}$ . In solving (4) the parameter  $a$  is hold constant at a small value, typically 1/1000, in consistency with (1), which requires  $\sqrt{d/h} \ll 1$  approximation, and so  $\nu$  is weakly dependent on  $a$ . To clarify this point, the parameter  $\nu$  is plotted as a function of the ratio  $r_2/r_1$  for three values of  $a = \sqrt{d/h}$  in Fig. 2, from which we see that the exponent  $\nu$  exhibits a weak dependence on  $a = \sqrt{d/h}$ , thus being primarily determined by the radii ratio  $r_2/r_1$ , especially when  $r_2/r_1 < 10$ . Equation (3) has been applied to examining several cavity configurations and the results compared with the frequencies calculated by the numerical code Superfish [20]. Almost coincident results have been obtained in many configurations, for which two representative cases are illustrated below.

First, a flat cavity with  $h < r_2 - r_1$  is displayed for two gap positions in Fig. 3, where the electric field lines emerging from the coaxial post all terminate in the closing disk at  $z = 1.5$  cm. The corresponding frequency curve plotted as function of  $d$  in Fig. 4 shows that the predicted and simulated resonant frequencies practically coincide over the whole range of gap variation. On the other hand, in the long cavity shown in Fig. 5 and for the intermediate gap spacing (Fig. 5(b)) the field lines originating from the lateral surface of the coaxial post now run to the outer cylinder, thus indicating that the electric field in the coaxial region is as strong as the field developed in the axial gap.

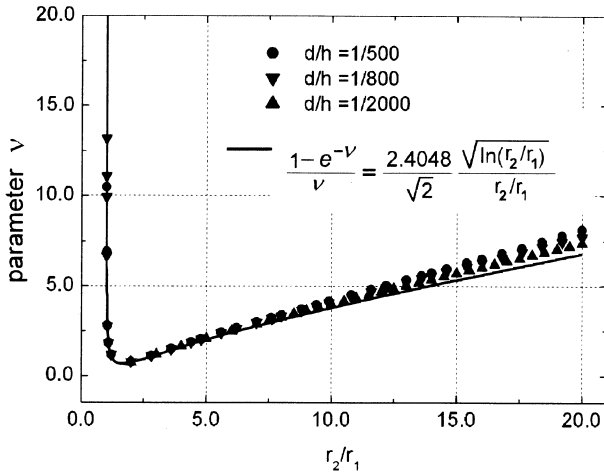


Fig. 2. Parameter  $\nu$  as a function of the radii ratio  $r_2/r_1$  for three values of  $a = \sqrt{d/h}$ . The solid line is obtained in the limit  $a\nu \ll 1$ , i. e., when the left-hand side of (4) reduces to  $[1 - \exp(-\nu)]/\nu$  and (4) becomes independent of  $a$ .

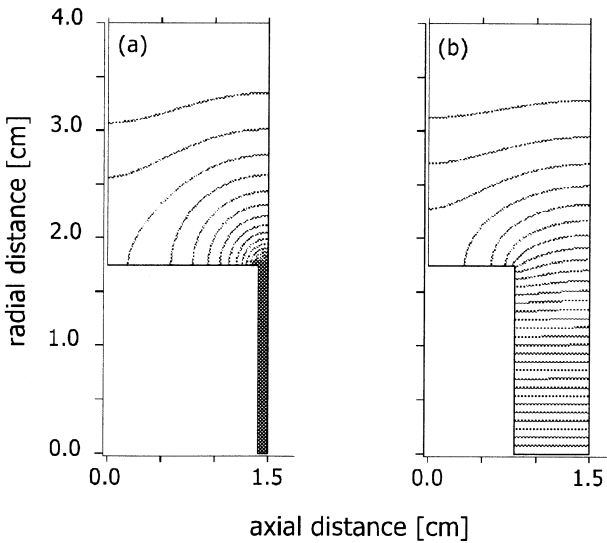


Fig. 3. Reentrant cylindrical cavities ( $r_2 = 4.00$  cm,  $r_1 = 1.75$  cm,  $h = 1.50$  cm) at axial gaps (a)  $d = 0.10$  cm, and (b)  $d = 0.70$  cm. The electric field lines shown are calculated with Superfish [1].

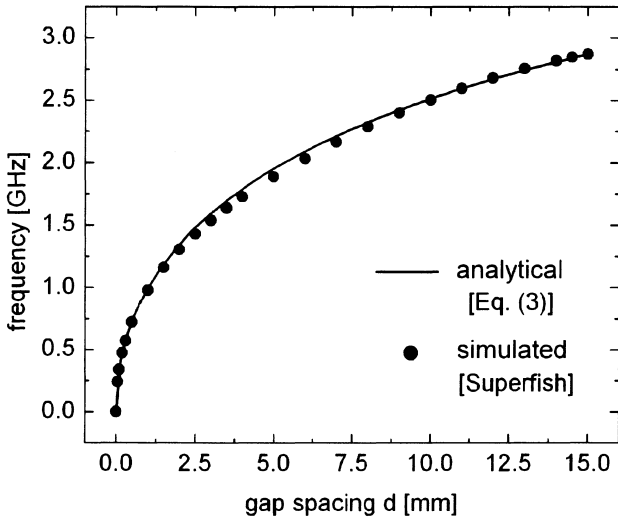


Fig. 4. Resonant frequency as function of gap  $d$  for the cavity in Fig. 3.

The comparative plot in Fig. 6 indicates that the predicted frequencies are several percent above the simulation values, within a 22.0% error at  $d=15.0$  mm. The reason for the discrepancy lies in the fact that long cavities ( $h>r_2-r_1$ ) are not gap controlled, in the sense that strong fields develop also in the coaxial region. Quantitatively, the radial electric field in a coaxial line is  $E_r=(E_0/r) \sin(2\pi z/\lambda_0)$ , where  $E_0$  is a constant; replacing the sine by its argument, the energy stored in the coaxial part ( $0\leq z\leq h-d$ ) of the cavity is estimated as

$$U_{coax} = \frac{\epsilon_0}{2} \int_{coax} E_r^2 dv = \frac{2\pi\epsilon}{6} \left(\frac{2\pi}{\lambda_0}\right)^2 E_0^2 (h-d)^3 \ln(r_2/r_1) \tag{5}$$

Similarly, the energy stored in the capacitor is estimated as  $U_{cap} = \epsilon_0 E_1^2 \pi r_1^2 d/2$  with the gap voltage  $E_1 d = E_0 (2\pi/\lambda)(h-d) \ln(r_2/r_1)$ . By using (1), we then arrive at

$$\frac{U_{coax}}{U_{cap}} = \frac{4\pi^2}{3} \frac{h(h-d)}{\lambda_0^2} \tag{6}$$

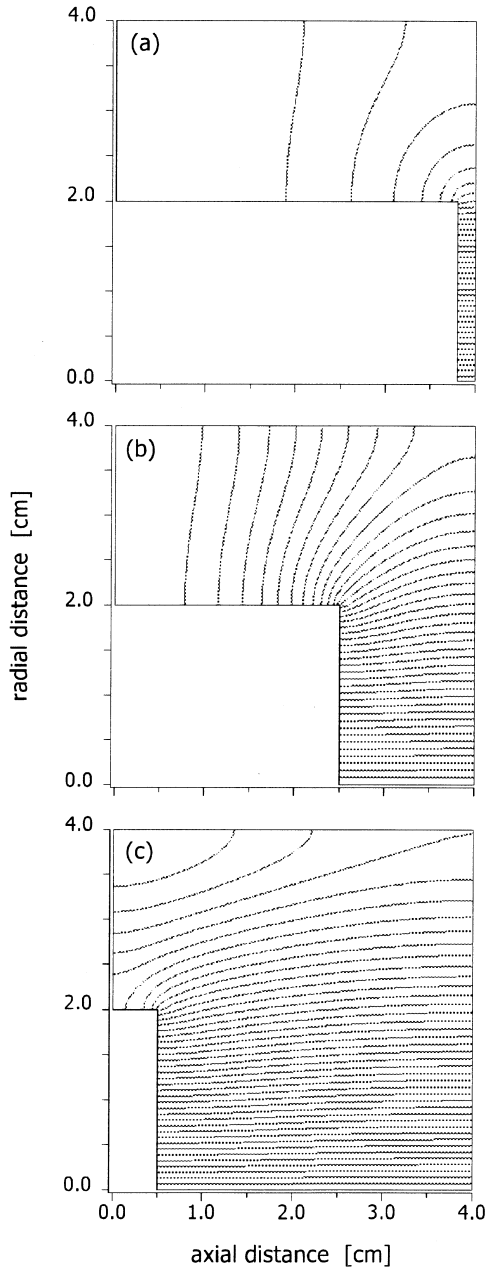


Fig. 5. Reentrant cylindrical cavities ( $r_2=4.00$  cm,  $r_1=2.00$  cm,  $h=4.00$  cm) for axial gaps (a)  $d=0.20$  cm, (b)  $d=1.50$  cm, and (c)  $d=3.50$  cm.

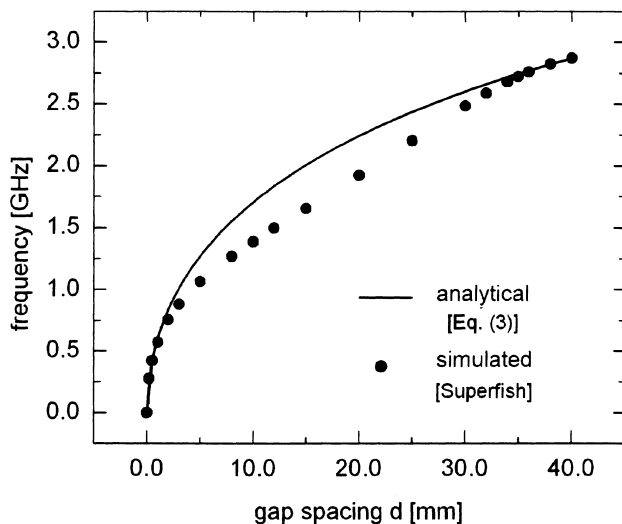


Fig. 6. Resonant frequency as function of gap  $d$  for the cavity in Fig. 5.

For the long cavity in Fig. 5(b), i. e.,  $h=4.00$  cm,  $r_2=4.00$  cm,  $r_1=2.00$  cm,  $d=1.50$ cm,  $\lambda_0=18.15$  cm ( $f=1.653$  GHz), the energy ratio (6) gives 0.40, meaning that the stored energy is shared in nearly equal parts between the coaxial and gap regions. But for the short cavity in Fig. 2(b),  $h=1.50$  cm,  $r_2=4.00$  cm,  $r_1=1.75$  cm,  $d=0.70$ cm,  $\lambda_0=13.85$  cm ( $f=2.165$  GHz) we get a small ratio of 0.08, which confirms that the short cavity is gap controlled. So the energy ratio (6) may be used as a criterion for the applicability of expression (3) over the full gap range  $0 \leq d \leq h$  and we conclusively say that for small gap  $d/h$  almost all the energy is stored in the capacitor, the condition for describing the cavity as a shunt LC circuit [13,16]. Within this context, the ohmic Q factor is expressed by  $Q = \omega CR_S$ , where  $R_S$  is the shunt resistance of the cavity at the gap

$$\frac{\omega^2 L^2}{R_S} = \frac{1}{2\pi\delta\sigma} \left( \frac{h-d}{r_1} + \frac{h}{r_1} + 2 \ln \frac{r_2}{r_1} \right) \quad (7)$$

with  $L = \mu_0(h/2\pi)\ln(r_2/r_1)$ ,  $\omega^2 = 1/LC$ ,  $\delta$  the skin depth, and  $\sigma$  the electrical conductivity, giving



$$\frac{1}{Q} = \delta \left( \frac{1}{h} + \frac{(h-d)/r_1 h + 1/r_2}{2\ln(r_2/r_1)} \right) \tag{8}$$

Then substituting  $f(d)$ , given by (3), in the skin depth expression  $\delta = 2/\sqrt{2\pi f(d)\mu_0\sigma}$ , we use (8) for calculating the Q for the cavity in Fig. 2, assuming a conductivity of  $\sigma = 5.7 \times 10^7 S/m$ . We see from Fig. 7 that the analytical calculation is in good agreement with the Superfish results.

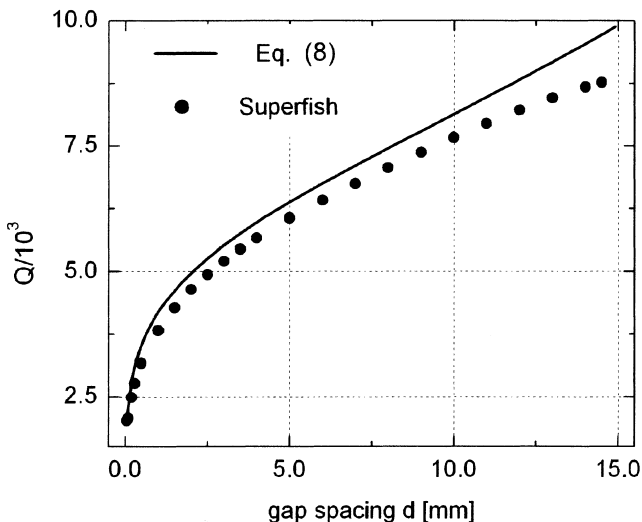


Fig. 7. For a conductivity  $\sigma = 5.7 \times 10^7 S/m$ , the ohmic Q factor as function of the axial gap for the cavity in Fig. 3.

### 3. Scaling and sensitivity $\Delta f/\Delta d$

We have discussed that in a flat cavity strong electric fields develop across the axial gap. This effect is particularly important in electromagnetic cavity-based transducers that operate at high fields to maximize the electrical coupling to an external mechanical transformer. A cavity of this sort finds advanced applications in parametric transducers to continually monitor the vibrational state of mass gravitational wave

antennas through modulation of the capacitive gap [12]. To address the frequency sensitivity to gap variations, we plot  $f(d)$  curves in Fig. 8 for three cavities with the same external radius  $r_2$ . Hence, the smaller the inner radius  $r_1$  and height  $h$ , the higher the sensitivity  $\Delta f/\Delta d$ , or tuning coefficient, which can be readily estimated from (3)

$$S(d) \equiv \frac{\Delta f}{\Delta d} = \frac{\chi}{4\pi} \frac{c}{r_2} \frac{1}{\sqrt{hd}} \frac{\nu \exp(-\nu\sqrt{d/h})}{1 - \exp(-\nu)} \tag{9}$$

giving, at  $d=0.1$  mm,  $S_1=5.3$  GHz/mm for cavity #1 for which  $\nu=7.64$ .

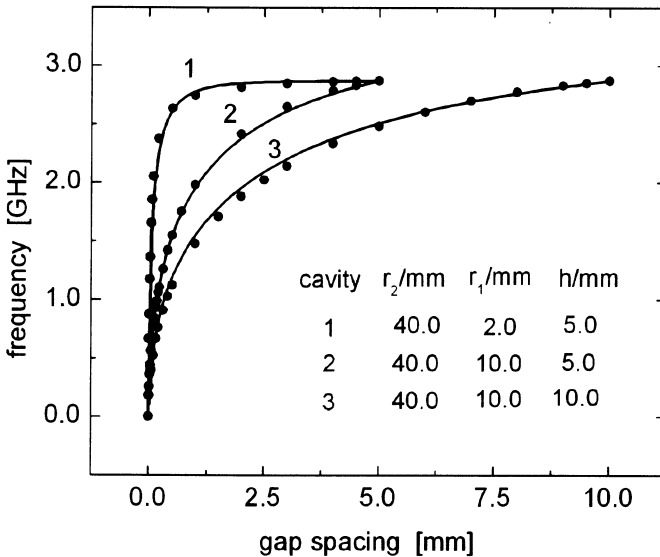


Fig. 8. Resonant frequency dependence upon  $gapd$  for three reentrant cavities. Filled circles denote Superfish results and the solid curves refer to analytical calculation from (3).

Since the parameter  $\nu$  increases with  $r_2/r_1$  and the rightmost term in (9) increases with  $\nu$  for  $d/h$  constant, then  $S(d)$  rises as  $r_2$  is reduced, with  $d/h$  and  $r_1$  held constant. For example, halving  $r_2$  in cavity #1 yields  $S(0.1 \text{ mm})= 5.9$  GHz/mm at the resonant frequency of 1.948 GHz. In addition, we infer from (3) that if a cavity is scaled down by a factor of 10, i.e. all the linear dimensions are divided by 10, then the resonant frequency will increase by a factor of 10 and, accordingly, the sensitivity will become

100 times as higher as in the lower-frequency cavity. Then, cavity #1 made ten times smaller (with a 10- $\mu\text{m}$  gap) will attain a sensitivity of 0.53 GHz/ $\mu\text{m}$  at the 18.97 GHz resonant frequency. Such illustrative examples demonstrate the usefulness of (3) in exploratory designs of reentrant cavities suitable for resonant-mass gravitational wave antennas [21], which require typical sensitivities of 1.0 GHz/ $\mu\text{m}$  to compensate for the sources of noise.

#### 4. Conclusion

The main feature of the reentrant cylindrical cavity relies on its ability to concentrate strong electric field in the gap space in conjunction with a wide tuning range, in which the resonant frequency  $f(d)$  decreases as the gap  $d$  shortens. This dependence makes the cavity a conveniently small resonator at a long wavelength. At a frequency of 2 GHz, for example, a  $\text{TE}_{101}$  rectangular cavity obtained by cutting a half guide wavelength section of a WR-430 waveguide (cross section 5.46 cm x 10.92 cm) would have a total length of 10.32 cm. This same resonant frequency could be operated by a reentrant cavity 8.00 cm in diameter and 1.50 cm long (Fig. 2), with a 0.54-cm gap yielding a sensitivity of 0.13 GHz/mm, with the smaller dimensions permitting an easy insertion of the cavity either in the gap of an electromagnet (for magnetic resonance spectroscopy) or into a Dewar vessel when using high-Q superconducting cavities.

The reentrant geometry makes it difficult to find an exact field solution inside the resonator. But on the basis of expressions for the frequency that are accurate enough near the limits of the gap interval, a unifying expression has been found to determine the resonant frequency over the full gap range. More accurate becomes the formalism as the cavity length gets smaller than the radial gap  $r_2 - r_1$ , meaning that the cavity is largely controlled by the axial gap in the sense that the electric-field lines emerging from the central post bend and converge towards the end plate. With a field configuration that resembles the  $\text{TM}_{010}$ -mode electric field pattern, the axial gap region is permeated by a well defined electric field, which makes such operating mode especially suitable for electromechanical transducers. The good agreement between analytical solutions and simulation results from the standard code Superfish [20] comes to demonstrate the usefulness of the proposed formalism in designing reentrant cavities for a wide range of applications.

## Acknowledgement

This work is supported by the National Council for Scientific and Technological Development (CNPq) and the State of São Paulo Research Foundation (FAPESP), Brazil.

## References

- [1] W. W. Hansen, "On the resonant frequency of closed concentric lines", *J. Appl. Phys.*, vol. 10, pp. 38-45, 1939.
- [2] E. L. Ginzton, and E. J. Nalos, "Shunt impedance of klystron cavities", *IRE Trans. Microwave Theory and Tech.*, vol. 3, no. 5, pp. 4-7, Oct. 1955.
- [3] S. Humphries, Jr., *Principles of Charged Particle Accelerators*, New York: Wiley, 1986.
- [4] A. J. C. Vieira, P. K. Herczfeld, A. Rosen, M. Ermold, E. E. Funk, W. D. Jennison, and K. J. Williams, "A mode-locked microchip laser optical transmitter for fiber radio", *IEEE. Trans. Microwave Theory Tech.*, vol. 49, no. 10, pp. 1882-1887, Oct. 2001.
- [5] M. Migliuolo, and G. Carter, "Novel tunable reentrant microwave cavity", *Rev. Sci. Instrum.*, vol. 59, no. 2, pp. 388-390, Feb. 1988.
- [6] F. Thompson, A. D. Haigh, B. M. Billon, and A. A. P. Gibson, "Analysis and design of a re-entrant microwave cavity for the characterization of single wheat grain kernels", *IEE Proc. Sci. Meas. Technol.*, vol. 150, no. 3, pp. 113-117, May 2003.
- [7] W. Xi, W. R. Tinga, W. A. G. Voss, and B. Q. Tian, "New results for coaxial re-entrant cavity with partially dielectric filled gap", *IEEE. Trans. Microwave Theory Tech.*, vol. 40, no. 4, pp. 747-752, April 1992.
- [8] F. Bordoni, L. Yinghua, B. Spatori, F. Felicangeli, F. Vasarelli, G. Cardarilli, B. Antonini, and R. Scrimaglio, "A microwave scanning surface harmonic microscope using a re-entrant resonant cavity", *Meas. Sci. Technol.* vol. 6, no. 8, pp.1208-1214, August 1995.
- [9] M. Giordano, F. Momo, and A. Sotgiu, "On the design of a re-entrant square cavity as resonator for low-frequency ESR spectroscopy", *J. Phys. E: Sci. Instrum.*, vol. 16, no.8, pp. 774-779, 1983.
- [10] G. P. Singh, M. Von Schickfus, and H. Maletta, "Spin-freezing process in spin-glasses", *Phys. Rev. Lett.*, vol. 51, no. 19, pp. 1791-1794, Nov. 1983.

- [11] H. S. Kim, and S. Ahn, "Numerical analysis of the C-band klystrode with annular electron beam", *Int. J. Infrared Millimeter Waves*, vol. 21, no. 1, pp. 11-20, Jan. 2000.
- [12] J. J. Barroso, P. J. Castro, O. D. Aguiar, and L. A. Carneiro, "Reentrant cavities as electromechanical transducers", *Rev. Sci. Instrum.*, vol. 75, no. 4, pp. 1000-1005, April, 2004.
- [13] J. C. Slater, *Microwave Electronics*, New York: Dover, 1969, pp.232-237.
- [14] E. Rivier and M. Vergé-Lapisardi, "Lumped parameters of a reentering cylindrical cavity", *IEEE Trans. Microwave Theory Tech.*, vol. 19, no. 3, pp. 309-214, March 1971.
- [15] H. E. Green, "The resonant frequency of a narrow-gap cylindrical cavity", *IEEE Trans. Microwave Theory Tech.*, vol. 25, no. 3, pp. 233-234, March 1977.
- [16] K. Fujisawa, "General treatment of klystron resonant cavities", *IRE Trans. Microwave Theory Tech.*, vol. 6, pp. 344-358, October 1958.
- [17] K. Uenakada, "Equivalent circuit of reentrant cavity", *IEEE Trans. Microwave Theory Tech.*, vol. 21, no. 1, pp. 48-51, January 1971.
- [18] A. G. Williamson, "120  
The resonant frequency and tuning characteristics of a narrow-gap reentrant cylindrical cavity", *IEEE. Trans. Microwave Theory Tech.*, vol. 24, no. 4, pp. 182-187, April 1976.
- [19] M. Jaworski, "On the resonant frequency of a reentrant cylindrical cavity", *IEEE Trans. Microwave Theory Tech.*, vol. 26, no. 6, pp. 256-260, April 1978.
- [20] J. H. Billen and L. M. Young, "Poisson/Superfish", Rep. LA -UR-96-1934, Los Alamos Nat. Lab., NM, 1996.
- [21] O. D. Aguiar, L. A. Andrade, J. J. Barroso, L. Camargo Filho, L. A. Carneiro, C. S. Castro, P. J. Castro, C. A. Costa, K. M. F. Co sta, J. C. N. de Araujo, A. U. de Lucena, W. de Paula, E. C. de Rey Neto, S. T. de Souza, A. C. Fauth, C. Frajuca, G. Frossati, S. R. Furtado, L. C. Lima, N. S. Magalhães, R. M. Marinho Jr., E. S. Matos, J. L. Melo, O. D. Miranda, N. F. Oliveira Jr., B. W. Paleo, M. Remy, K. L. Ribeiro, C. Stellati, W. F. Velloso Jr., J. Weber, "The Brazilian spherical detector: progress and plans", *Classical and Quantum Gravity*, vol. 21(5), pp. S457-S463, March 2004.